Available online at www.sciencedirect.com
ScienceDirect
Deep-Sea Research I 53 (2006) 1616–1634
DEEP-SEA RESEARCH PART I
www.elsevier.com/locate/dsr

Vertical distribution of phytoplankton biomass, production and growth in the Atlantic subtropical gyres

Valesca Pérez[a,*], Emilio Fernández[a], Emilio Marañón[a], Xosé Anxelu G. Morán[b], Mike V. Zubkov[c]

[a]*Departamento de Ecología y Biología Animal, Facultad de Ciencias del Mar, Universidad de Vigo, Ctra. Colexio Universitario s/n, 36310 Vigo, Spain*
[b]*Instituto Español de Oceanografía, Centro Oceanográfico de Xixón, Camín de L'Arbeyal, s/n, E 33212 Xixón, Spain*
[c]*George Deacon Division for Ocean Processes, Southampton Oceanography Centre, University of Southampton, Southampton SO14 3ZH, UK*

Received 26 October 2005; received in revised form 28 July 2006; accepted 31 July 2006
Available online 2 October 2006

Abstract

Ninety-four stations were sampled in the Atlantic subtropical gyres during 10 cruises carried out between 1995 and 2001, mainly in boreal spring and autumn. Chlorophyll *a* (Chl-*a*) and primary production were measured during all cruises, and phytoplankton biomass was estimated in part of them. Picoplankton ($<2\,\mu m$) represented $>60\%$ of total Chl-*a* concentration measured at the surface, and their contribution to this variable increased with depth. Phytoplankton carbon concentrations were higher in the upper metres of the water column, whereas Chl-*a* showed a deep maximum (DCM). At each station, the water column was divided into the upper mixed layer (ML) and the DCM layer (DCML). The boundary between the two layers was calculated as the depth where Chl-*a* concentration was 50% of the maximum Chl-*a* concentration. On average DCML extends from 67 to 126 m depth. Carbon to Chl-*a* (C:Chl-*a*) ratios were used to estimate phytoplankton carbon content from Chl-*a* in order to obtain a large phytoplankton carbon dataset. Total C:Chl-*a* ratios averaged ($\pm$s.e.) 103 ± 7 ($n=22$) in the ML and 24 ± 4 ($n=12$) in the DCML and were higher in larger cells than in picoplankton. Using these ratios and primary production measurements, we derived mean specific growth rates of $0.17\pm0.01\,d^{-1}$ ($n=173$) in the ML and $0.20\pm0.01\,d^{-1}$ ($n=165$) in the DCML although the differences were not significant (*t*-test, $p>0.05$). Our results suggest a moderate contribution of the DCML (43%) to both phytoplankton biomass and primary production in the Atlantic subtropical gyres.

Keywords: Phytoplankton; Biomass; Primary production; Growth; Atlantic subtropical gyres; AMT

1. Introduction

The deep chlorophyll maximum (DCM) is a consistent oceanographic feature of tropical and subtropical oceans. Several mechanisms have been proposed to explain its formation and maintenance, including higher in-situ growth at the nutricline

*Corresponding author. Tel.: +34 986 81 40 87; fax: +34 986 81 25 56.
E-mail address: vperez@uvigo.es (V. Pérez).

0967-0637/$ - see front matter © 2006 Elsevier Ltd. All rights reserved.
doi:10.1016/j.dsr.2006.07.008

than in the upper mixed layer, physiological acclimation to low irradiance and high nutrient concentrations, accumulation of sinking phytoplankton at density gradients, behavioural aggregation of phytoplankton groups, and differential grazing on phytoplankton (e.g. Cullen, 1982; Gould, 1987).

In the subtropical gyres, the DCM has been suggested to be the result of a physiological acclimation of phytoplankton to low light levels in the presence of high nutrient concentrations (Cullen,1982) resulting in an increase in cellular chlorophyll *a* (Chl-*a*) content and, consequently, in a decrease in the carbon to Chl-*a* (C:Chl-*a*) ratio. These areas, considered as the oligotrophic extreme of the "typical tropical structure" (TTS) regions described by Herbland and Voituriez (1979), are characterised by an upper mixed layer, where nutrients are usually undetectable, a light-limited deep layer, and the presence of a Chl-*a* maximum located in the vicinity of the nutricline. In the subtropical gyres, therefore, the use of Chl-*a* concentration as an indicator of phytoplankton biomass could very likely result in the false identification of the DCM as a carbon-biomass maximum.

Studies based on Chl-*a* size fractionation (Herbland et al., 1985; LeBouteiller et al., 1992) show that in areas characterised by the TTS, the contribution of small phytoplankton cells to total Chl-*a* is higher in surface waters and decreases with depth, reaching 50% at the DCM. However, studies based on flow cytometry show that the slope of the size-abundance spectrum, which is a log–log plot of cell abundance (*y*-axis) versus cell size (*x*-axis), becomes more negative from surface to the DCM and then increases with depth. These results reveal a growing importance of small phytoplankton cells at the DCM and a progressive change toward larger cells underneath (Gin et al., 1999), and they suggest that the phytoplankton community structure shows significant vertical variability in oligotrophic environments. Species, pigment analyses and flow-cytometry studies reveal a two-layered structure of the phytoplankton composition in the tropical and subtropical Atlantic and Pacific (Gieskes and Kraay, 1986; Ondrusek et al., 1991; Venrick 1999; Veldhuis and Kraay, 2004). Usually, Prochlorophytes and Cyanophytes dominate the upper mixed layer while pico and nanoeukaryotes constitute a high portion of phytoplankton biomass at the DCM. In terms of abundance, *Prochlorococcus* dominates the picophytoplankton community throughout the water column in tropical and subtropical oceans (Campbell and Vaulot, 1993; Partensky et al., 1996; Zubkov et al., 1998). However, *Prochlorococcus* dominance in terms of cell numbers does not always translate into a parallel dominance in terms of biomass (Claustre and Marty, 1995; Barlow et al., 2002; Veldhuis and Kraay, 2004).

Primary production rates measured in the gyres (Letelier et al., 1996; Marañón et al., 2000) are higher in the upper metres of the water column. Moreover, small differences (less than 10%) have been observed in satellite-derived primary production estimates of the North Atlantic and Pacific subtropical gyres, depending on whether parameterized or uniform Chl-*a* profiles are used (Sathyendranath et al., 1995; Ondrusek et al., 2001). These results suggest a relatively low contribution of the DCM to depth-integrated primary production. Equally, phytoplankton turnover rates are generally higher in the upper mixed layer than in the proximity of the DCM (Malone et al., 1993; Goericke and Welschmeyer, 1998; Quevedo and Anadón, 2001), although a large variability in growth rate, ranging from 0.15 to 1.3 d^{-1}, has been reported in the subtropical gyres (e.g., Marañón, 2005), revealing the existence of a more dynamic environment in the upper mixed layer of the oligotrophic oceans.

Most previous analyses of the vertical variability of phytoplankton biomass, production and size structure in the subtropical ocean have been based on a relatively small number of observations, or have limited spatial or temporal coverage. A recent study (Teira et al., 2005) aimed to characterise the temporal and spatial variability of primary production and Chl-*a* in the northeastern subtropical Atlantic based on observations collected for 12 years in the region. In the present study, we use part of the Teira et al. data together with data from the South Atlantic subtropical gyre to obtain a large dataset (>90 stations) of total and size-fractionated Chl-*a* and primary production, together with phytoplankton C biomass measured in the North and South Atlantic subtropical gyres on 10 cruises conducted during different seasons from 1995 to 2001. While Teira et al. (2005) focussed on the temporal and spatial variability, we used this extensive dataset to characterize the patterns of phytoplankton vertical variability in the subtropical gyres. In order to assess the biogeochemical and

ecological role that the DCM plays in the oligotrophic ocean, we aim to answer the following specific questions: (1) How does phytoplankton size structure change with depth? (2) Is the DCM a phytoplankton biomass maximum? (3) Is the DCM a productivity maximum? and (4) Do phytoplankton grow faster at the DCM than in surface water?

2. Methods

Sampling was carried out at 94 oligotrophic stations (surface chlorophyll $<0.2\,\mathrm{mg\,m^{-3}}$, undetectable surface nitrate concentration, sharp thermocline) of the subtropical gyres of the Atlantic Ocean during 10 cruises conducted from 1995 to 2001 (Fig. 1, Table 1). Fifty-five stations were

Fig. 1. Location of sampling stations over SeaWiFS September 1997–August 2000 Chl-*a* composite.

Table 1
Summary of cruises conducted from 1995 to 2001 in the subtropical NE Atlantic (NASTE) and in the subtropical S Atlantic (SATL) Ocean where the results presented in this study were obtained

Cruise	Ship	NASTE St	Dates NASTE	SATL St	Dates SATL
AMT-1	RRS James Clark Ross	3	30/09–03/10 (1995)	4	12/10–15/10 (1995)
AMT-2	RRS James Clark Ross	3	14/05–16/05 (1996)	4	04/05–07/05 (1996)
AMT-3	RRS James Clark Ross	2	28/09–29/09 (1996)	7	07/10–13/10 (1996)
AMT-4	RRS James Clark Ross	3	16/05–18/05 (1997)	5	02/05–08/05 (1997)
AMT-5	RRS James Clark Ross	2	26/09–27/09 (1997)	5	05/10–09/10 (1997)
AMT-6	RRS James Clark Ross	2	08/06–09/06 (1998)		
Azores-1	BIO Hespérides	4	02/08–05/08 (1998)		
Azores-2	BIO Hespérides	27	08/04–17/04 (1999)		
AMT-11	RRS James Clark Ross	5	18/09–20/09 (2000)	14	01/10–08/10 (2000)
CIRCANA-1	BIO Hespérides	4	30/10–2/11 (2001)		

Number of stations (St) and sampling dates are indicated for each cruise.

sampled in the eastern North Atlantic subtropical gyre between 20° and 35°N and 39 stations in the South Atlantic gyre between 5° and 30°S. Hereafter, we shall use the terms NASTE and SATL to refer the two areas, although we are aware that they do not include the whole extension of the provinces as described by Longhurst (1998). Sampling was conducted between 1000 and 1200 local time, except during AMT-11, when two stations were sampled daily predawn and at noon. All chemical and microbiological measurements from AMT-11 presented here were carried out on water collected during the early morning stations, except for Chl-*a* concentration, which was measured on every station.

During AMT cruises, vertical profiles of photosynthetically active irradiance (PAR, 400–700 nm) were obtained by integrating the measurements of downwelling irradiance at seven SeaWiFS wavelength bands as measured with an optical profiler (SeaOPS). The downwelling irradiance in the water column was determined with a Licor Li-1800UW spectroradiometer during Azores cruises and with a Satlantic OCP-100 FF sensor during the CIRCANA-1 cruise. Vertical profiles of temperature and salinity were obtained at each station with a CTD probe attached to a rosette sampler equipped with Niskin bottles. CTD temperature and salinity sensors were calibrated with digital reversing thermometers and water samples drawn for salinity determinations. In this study the beginning of the thermocline was defined as the depth where the thermal gradient was $>0.1\,^{\circ}C/m$. Sampling strategy and the acquisition of complementary physical and chemical variables followed JGOFS protocols (http://www.uib.no/jgofs/Publications/Report_Series/), although there were slight variations on some of the cruises.

During Azores-1, Azores-2 and AMT cruises, dissolved inorganic nitrogen was determined with a Technicon segmented flow colorimetric auto-analyzer as described in Tréguer and LeCorre (1975) (Azores-1 and Azores-2 cruises) and in Woodward (1994) (AMT cruises). Nitrate detection limits range from 25 nM during the AMT-11 cruise to 0.1 μM during the rest of the AMT cruises. The nitracline depth was considered as the first depth where nitrate values were detectable.

Sampling depths for Chl-*a* and primary production were determined after examination of the irradiance, temperature, salinity and fluorescence profiles. Typically, 2–3 sampling depths were located in the upper mixed layer, 2–3 in the DCM zone, and 1–2 below the DCM. Water samples (100–250 ml) for Chl-*a* determination were collected from 5–7 depths in the upper 200 m of the water column and sequentially filtered through 20, 2 and 0.2 μm polycarbonate filters. Chl-*a* concentration was measured fluorometrically after extraction in 90% acetone at $-20\,^{\circ}C$ overnight. During AMT-1 and AMT-2 cruises the acidification technique of Holm-Hansen et al. (1965) was used. During the rest of the cruises Chl-*a* concentration was measured by the non-acidification technique of Welschmeyer (1994). Total Chl-*a* was determined from the addition of size-fractionated measurements. During AMT-1, only total, unfractionated Chl-*a* was measured. All stations were characterised by the existence of a deep (>50 m depth) chlorophyll maximum where the Chl-*a* concentration was at least twice the surface value. At each station, the

boundary between the low Chl-*a* upper mixed layer (ML) and the DCM layer (DCML) was chosen as the depth where Chl-*a* concentration was 50% of the maximum Chl-*a* concentration. This concentration also defined the bottom of the DCML, which, on average, extended from 67 to 126 m depth.

During AMT-1, AMT-2, AMT-3, and AMT-4, 100 ml samples were preserved with Lugol's solution for identification to species level and counting of nano- (2–20 μm) and microplankton (>20 μm). At least two samples, one from surface and the other from the DCM, were taken at each station. Samples were allowed to settle in sedimentation chambers for 2–3 d and subsequently examined at 187 and 750 magnifications under an inverted microscope. Cell numbers were converted into carbon biomass as described by Holligan et al. (1984). The abundance of phototrophic picoplankton (<2 μm) was determined with a flow cytometer (Zubkov et al., 1998; Morán et al., 2004) during AMT-3, AMT-4, and CIRCANA-1 cruises. *Synechococcus* spp. and *Prochlorococcus* spp. cyanobacteria, and small photosynthetic eukaryotes (picoeukaryotes) were discriminated. Samples were taken at 10–12 depths from the surface down to 200 m. Picoplankton abundance was transformed to biomass with the empirical conversion factors obtained by Zubkov et al. (2000): 32 fgC cell^{-1} for *Prochlorococcus* spp., 103 fgC cell^{-1} for *Synechococcus* spp. and 1496 fgC cell^{-1} for picoeukaryotes.

For the determination of primary production, water samples from five to seven depths were transferred, immediately after collection, to four 75-ml acid-cleaned polystyrene bottles (3 light and 1 dark), inoculated with 370–740 kBq (10–20 μCi) $NaH^{14}CO_3$ and incubated for 6–7 h. Incubations were started within 30 min of sampling and were terminated at sunset, except during AMT-11, when incubations lasted 24 h. Samples were placed in an on-deck incubator that simulated the irradiance at the original sampling depths and were cooled with surface seawater. Average temperature difference between surface and the DCM depth was 2.5 °C. Temperature difference was higher than 5 °C at 13 of the 94 stations. After the incubation period, samples were sequentially filtered through 20, 2, and 0.2 μm polycarbonate filters at very low vacuum (<50 mm Hg). During AMT-1 only total primary production was estimated by filtration through glass fibre filters. Removal of inorganic ^{14}C that had not been incorporated by phytoplankton as organic carbon from the filters was achieved by exposing them to concentrated hydrochloric acid (HCl) fumes for 12 h. Then the filters were transferred to scintillation vials to which 4 ml of scintillation cocktail were added. Radioactivity in each sample was measured on a scintillation counter on board (AMT cruises, Azores-2 and CIRCANA-1) or ashore (Azores-1). Quenching was corrected with an external standard. Dark-bottle values were subtracted from the counts obtained in the light samples. Total primary production was determined by addition of the size fractionated rates. Daily rates were calculated by taking into account the daylight period and assuming that dark respiratory losses amount to 20% of the carbon incorporation during the light period (Marra and Barber, 2004).

Euphotic-zone-integrated values of size-fractionated and total Chl-*a* and particulate carbon production were obtained by trapezoidal integration of the volumetric data down to the depth of 1% surface incident irradiance.

3. Results

3.1. The DCM in the subtropical gyres

Table 2 shows averaged values of selected physical, chemical and biological variables in the subtropical gyres during the present study. Nitracline depth was similar in the NASTE and the SATL (*t*-test, $p>0.05$), while the thermocline was significantly deeper in the SATL than in the NASTE (*t*-test, $p<0.001$). The depth of the DCM was also significantly higher in the SATL (*t*-test, $p<0.001$). Mean temperature difference between the DCM depth and surface was 2.29 °C in the NASTE and 2.70 °C in the SATL. Chl-*a* concentrations were <0.1 and <0.4 mg m^{-3} at the surface and at the DCM, respectively, and slightly higher Chl-*a* concentrations were measured in the SATL as compared to the NASTE at the surface (*t*-test, $p<0.001$) and at the DCM (*t*-test, $p<0.05$). Euphotic-depth-integrated primary production rates and picoplankton (<2 μm) contributions to total primary production showed no differences between the two gyres (*t*-test, $p>0.05$). On the contrary, depth-integrated Chl-*a* concentrations and picoplankton contributions to total Chl-*a* were significantly higher in the SATL than in the NASTE (*t*-test, $p<0.001$), although the differences in total Chl-*a* between gyres disappeared upon division by the euphotic-layer depth. Picophytoplankton contribution to Chl-*a* was

Table 2
Averaged values ± standard error (s.e.) and sample size (n) of selected variables at the sampling stations

	NASTE	SATL	Total
Latitude	20°N–35°N	5°S–30°S	20°N–35°N 5°S–30°S
Thermocline depth (m)	51 ± 5 (24)	113 ± 6 (39)	89 ± 6 (63)
Nitracline depth (m)	123 ± 5 (45)	136 ± 6 (34)	128 ± 4 (79)
DCM depth (m)	93 ± 3 (55)	119 ± 4 (39)	104 ± 3 (94)
Surface Chl-*a* ($mg\,m^{-3}$)	0.06 ± 0.01 (55)	0.09 ± 0.01 (39)	0.07 ± 0.00 (94)
DCM ($mg\,m^{-3}$)	0.29 ± 0.01 (55)	0.34 ± 0.02 (39)	0.31 ± 0.01 (94)
Integrated Chl-*a* ($mg\,m^{-2}$)	17 ± 1 (55)	23 ± 1 (39)	19 ± 1 (94)
Integrated primary production ($mg\,C\,m^{-2}\,d^{-1}$)	156 ± 16 (36)	205 ± 17 (33)	180 ± 12 (69)
Contribution of <2 μm cells to total Chl-*a* (%)	71 ± 1 (52)	79 ± 1 (32)	74 ± 1 (84)
Contribution of <2 μm cells to total primary production (%)	51 ± 2 (33)	54 ± 3 (25)	52 ± 2 (58)

significantly larger than to primary production (*t*-test, $p<0.001$).

3.2. Chl-a and phytoplankton carbon biomass (Phyto C)

The averaged vertical distribution of Chl-*a* concentration measured in the subtropical gyres (NASTE + SATL; Fig. 2a) remained almost constant in the upper 50 m of the water column, then Chl-*a* concentration increased progressively down to the DCM, located at 80–110 m, where maximum values of $\sim 0.26\,mg\,m^{-3}$ were reached. Chl-*a* concentrations decreased steadily from the DCM down to 200 m depth. A very similar averaged vertical Chl-*a* distribution was found in each gyre separately (Figs. 2b and c), although in the SATL Chl-*a* concentrations at the DCM were higher. By contrast, the vertical distribution of total phytoplankton carbon biomass (Phyto C) (Figs. 2d–f) presented higher concentrations ($\sim 10\,mg\,m^{-3}$) in the upper 90 m of the water column and decreased to $\sim 5\,mg\,m^{-3}$ in the lower part of the DCML. However, it is difficult to get a real trend given the scarce number of Phyto C measurements.

The contribution of picoplankton to total Chl-*a* was always higher than 60% (Fig. 3a) and increased from 60% at the surface to 80% at 160 m depth. A similar pattern was observed in the NASTE (Fig. 3b), where higher percentages were observed at 130 m (75%). In the SATL (Fig. 3c), the trend was slightly different. The contribution of picoplankton to total Chl-*a* increased from 72% at the surface to 90% at 200 m, although a subsurface maximum (~80%) was present at 20–30 m. The contribution of picoplankton to Phyto C ranged from 38% to 63% (Figs. 3d–f) and did not show a clear vertical pattern.

Averaged (± s.e.) Chl-*a* and Phyto C values in the ML (whose lower boundary is defined as the depth where Chl-*a* concentration is 50% of the maximum Chl-*a* concentration; see Section 2) and in the DCML are shown in Table 3. Very low Chl-*a* concentrations were measured in the ML. Total, unfractionated Chl-*a* concentrations ranged from 0.01 to $0.23\,mg\,m^{-3}$ in the ML and from 0.05 to $0.64\,mg\,m^{-3}$ in the DCML. Chl-*a* concentration was also low in the larger (>2 μm) phytoplankton size fraction as picophytoplankton (<2 μm) dominates Chl-*a* concentrations throughout the water column (Fig. 3a). On the contrary, averaged Phyto C concentration was similar in the ML and in the DCML (*t*-test, $p>0.05$) and was significantly higher in the small than in the large size fraction (*t*-test, $p<0.001$).

We calculated C:Chl-*a* ratios using total and size-fractionated Phyto C and Chl-*a* concentrations measured in both gyres during AMT-3 and AMT-4 cruises, when size-fractionated Chl-*a* and Phyto C were measured simultaneously. The datasets from both hemispheres were pooled together, given the scarce number of Phyto C measurements available and the relatively constant vertical pattern followed by Chl-*a* and Phyto C in the two gyres (see Fig. 2). Ratios >500 were excluded from the analysis (4 values). Total C:Chl-*a* ratios ranged from 56 to $200\,mg\,C\,mg\,Chl^{-1}$ in the ML and from 11 to $54\,mg\,C\,mg\,Chl^{-1}$ in the DCML. Size-fractionated C:Chl-*a* ratios in the ML ranged between 47 and 155 for <2 μm phytoplankton, and between 74 and 493 for the >2 μm. In the DCML, C:Chl-*a* ratios varied between 8 and 30 in the <2 μm size fraction and between 29 and 147 in the >2 μm size fraction. Averaged C:Chl-*a* ratios (Table 3) were significantly higher in the ML than in the DCML and in the

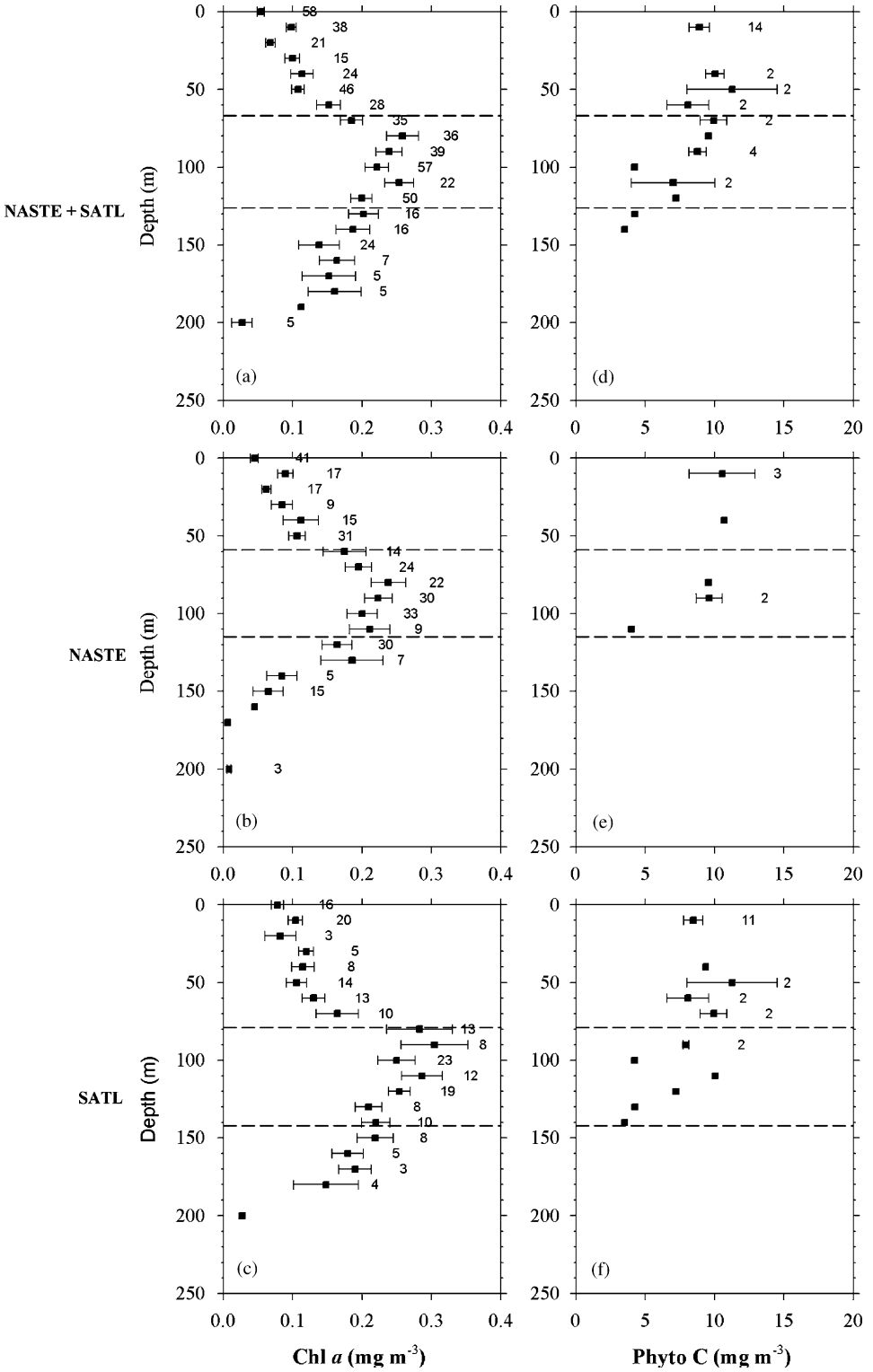

Fig. 2. Averaged vertical profiles of total Chl-*a* (left panels) and total Phyto C (right panels), both in mg m^{-3}, at all sampling stations (a and d), at the stations located in the Northern gyre (b and e) and at the stations located in the Southern gyre (c and f). Horizontal bars represent the standard error (s.e.). Numbers indicate the number of values making up each average. No number (or error bar) indicates only a single value. Dashed lines represent the vertical limits of the DCML.

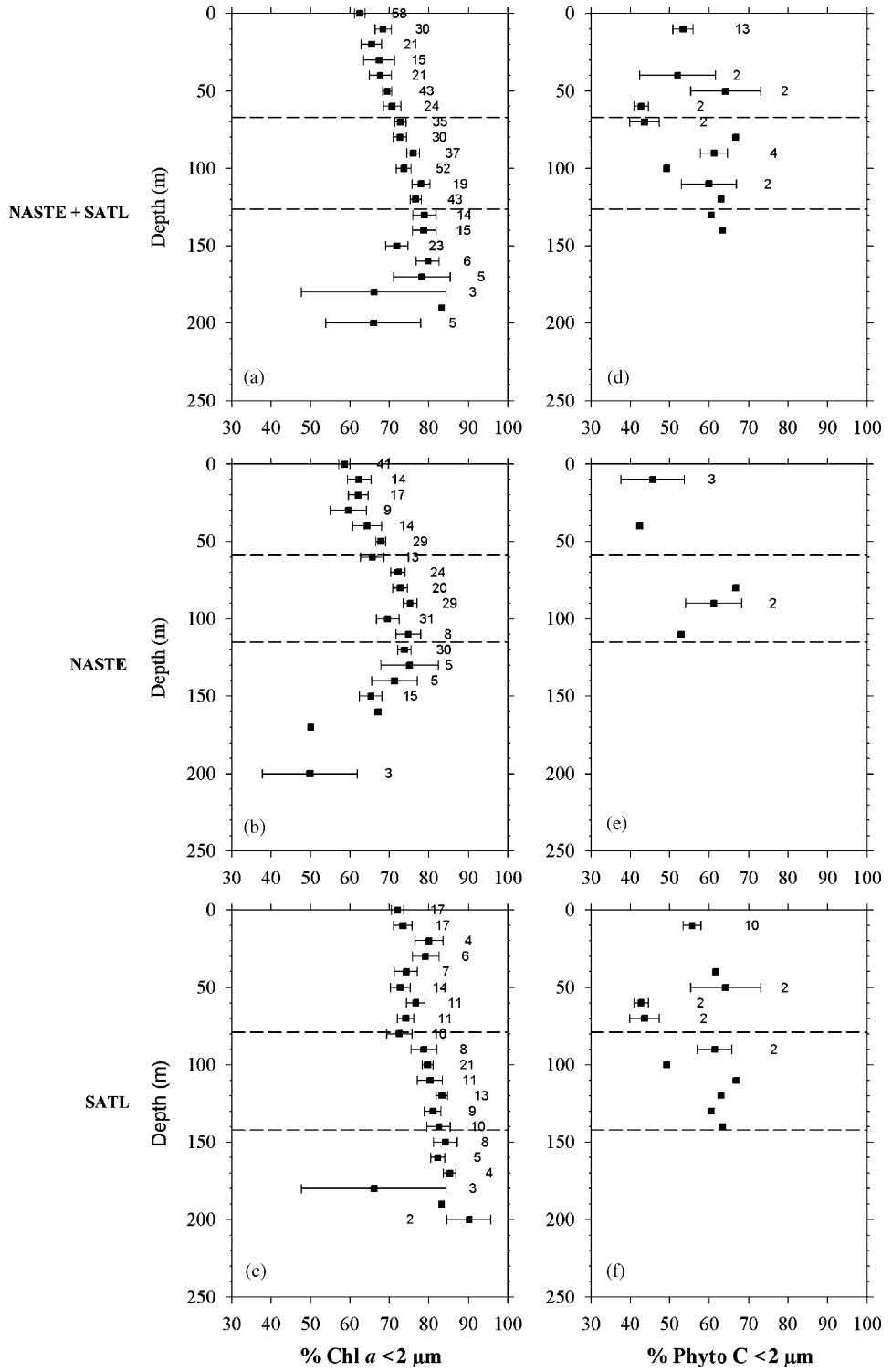

Fig. 3. Averaged vertical profiles of the picoplankton contribution (%) to total Chl-*a* (% Chl-*a* <2 µm; left panels) and to total Phyto C (% Phyto C <2 µm; right panels) at all sampling stations (a and d), at the stations located in the Northern gyre (b and e) and at the stations located in the Southern gyre (c and f). Horizontal bars represent the standard error (s.e.). Numbers indicate the number of values making up each average. No number (or error bar) indicates only a single value. Dashed lines represent the vertical limits of the DCML.

Table 3
Averaged values ± standard error (s.e.) and data number (n) of selected variables in the mixed layer (ML) and in the DCM layer (DCML) for each size fraction

	Total fraction		<2 μm fraction		>2 μm fraction	
	Upper layer	DCM layer	Upper layer	DCM layer	Upper layer	DCM layer
Chl-*a* ($mg\,m^{-3}$)	0.09 ± 0.00 (237)	0.25 ± 0.01 (244)	0.06 ± 0.00 (223)	0.19 ± 0.01 (215)	0.03 ± 0.00 (222)	0.05 ± 0.00 (218)
Phyto C ($mg\,m^{-3}$)	9.6 ± 0.7 (22)	7.3 ± 0.8 (12)	6.0 ± 0.3 (83)	5.8 ± 0.4 (72)	4.2 ± 0.3 (38)	3.2 ± 0.3 (29)
C:Chl-*a* ratio ($mg\,C\,mg\,Chl^{-1}$)	103 ± 7 (22)	24 ± 4 (12)	77 ± 6 (22)	17 ± 2 (12)	186 ± 21 (22)	58 ± 10 (12)
Est Phyto C ($mg\,m^{-3}$)	9.0 ± 0.3 (237)	6.0 ± 0.2 (244)	4.5 ± 0.2 (223)	3.3 ± 0.1 (215)	4.9 ± 0.2 (222)	2.9 ± 0.1 (218)
Primary production ($mg\,m^{-3}\,d^{-1}$)	1.68 ± 0.09 (180)	1.39 ± 0.09 (170)	0.81 ± 0.05 (166)	0.99 ± 0.07 (141)	0.92 ± 0.06 (164)	0.51 ± 0.04 (142)
μ (d^{-1})	0.17 ± 0.01 (173)	0.20 ± 0.01 (165)	0.17 ± 0.01 (160)	0.25 ± 0.02 (136)	0.17 ± 0.01 (155)	0.18 ± 0.01 (137)

For abbreviations see text.

>2 μm than in the <2 μm size fraction (*t*-test, $p<0.001$). We estimated the phytoplankton carbon biomass (Est Phyto C) for each layer by multiplying the average Chl-*a* concentration by the averaged C:Chl-*a* estimated for each layer. Unlike the measured Phyto C biomass, Est Phyto C concentrations were significantly higher in the ML than in the DCML (*t*-test, $p<0.001$) in all size fractions. Est Phyto C was also higher in the <2 μm size fraction than in large size fraction in the DCML (*t*-test, $p<0.05$), although there was no difference between the two size fractions in the ML.

3.3. Vertical variability of phytoplankton primary production and growth rates

Averaged vertical profiles of primary production, when both gyres are jointly considered (Fig. 4a), showed higher total C incorporation rates in the upper 90 m of the water column (ranging from 1.0 to 2.3 $mg\,m^{-3}\,d^{-1}$) than in the DCML. However, this pattern is slightly different in each gyre. In the northern gyre (Fig. 4b), the highest primary production rates (up to 2.2 $mg\,m^{-3}\,d^{-1}$) were measured in the upper 40 m, while in the southern gyre (Fig. 4c) the highest rates (up to 2.7 $mg\,m^{-3}\,d^{-1}$ at 80 m) were found in the upper part of the DCML. In general, the contribution of picoplankton to primary productivity (Fig. 4d) showed a slight increase with depth from ~45% in the upper 60 m of the water column to ~60% at 120 m. Below this depth, picoplankton contribution to primary production decreased. This trend mirrored that of the northern gyre (Fig. 4e), while in the southern gyre (Fig. 4f) picoplankton contributions reached higher values than in the NASTE. Averaged primary production measured in the ML (Table 3) was significantly different from that averaged in the DCML (*t*-test, $p<0.05$ for total and the <2 μm size fraction and $p<0.001$ for the >2 μm size fraction). Primary production rates were higher in the ML for large (>2 μm) and total phytoplankton sizes and in the DCML for the small (<2 μm) cells.

We calculated the carbon-specific phytoplankton growth rate (μ, d^{-1}) from daily primary production rates (ΔC) and the estimated phytoplankton carbon biomass (Est Phyto C) according to the equation: $\mu = \ln[(\text{Est Phyto C} + \Delta C)/\text{Est Phyto C}]$. We have chosen estimated phytoplankton biomass (Est Phyto C) instead of measured phytoplankton biomass (Phyto C) because of the scarcity of Phyto C data available (see Figs. 2 and 3). The carbon specific phytoplankton growth rate showed almost constant values (~0.20 d^{-1}) from surface to 110 m, then decreased with depth (Fig. 5a). In the NASTE, μ showed values >0.20 d^{-1} both in the ML and in the DCML (Fig. 5b), while in the southern gyre the highest rates (>0.20 d^{-1}) were found at 80–90 m depth coinciding with the beginning of the DCML (Fig. 5c). The highest picoplankton growth rates were estimated at 70–80 m depth (~0.30 d^{-1}), when the two gyres were either jointly or separately considered (Figs. 5d–f). Relatively high picoplankton μ values (up to 0.27 d^{-1}) were also estimated for the upper water column in the northern gyre (Fig. 5e). It is worth mentioning the large variability associated with picoplankton growth rate estimates. In the case of >2 μm phytoplankton (Figs. 5g–i), the highest growth rates were measured in the upper 40 m of the water column, reaching 0.23 and 0.35 d^{-1} in the NASTE and the SATL, respectively, and decreasing rapidly downwards. Averaged phytoplankton growth rates in the ML and in the DCML did not differ (*t*-test, $p>0.05$, Table 3). However, significant differences were found in the small size fraction between the two layers. As for

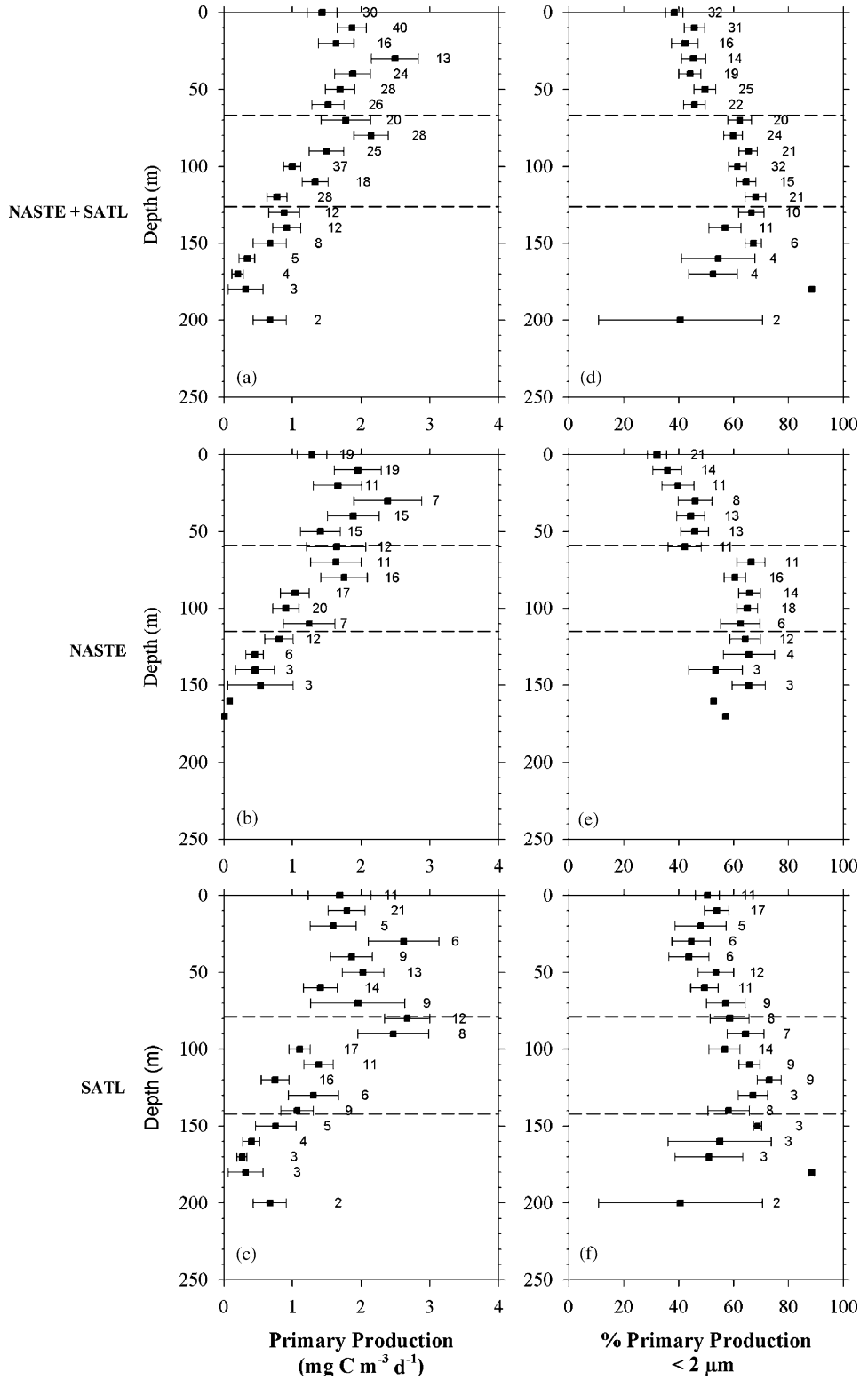

Fig. 4. Averaged vertical profiles of total primary production rates in $mg\,m^{-3}\,d^{-1}$ (left panels) and picoplankton contribution to total primary production expressed as percentage (right panels) at all sampling stations (a and d), at the stations located in the Northern gyre (b and e) and at the stations located in the Southern gyre (c and f). Horizontal bars represent the standard error (s.e.). Numbers indicate the number of values making up each average. No number (or error bar) indicates only a single value. Dashed lines represent the vertical limits of the DCML.

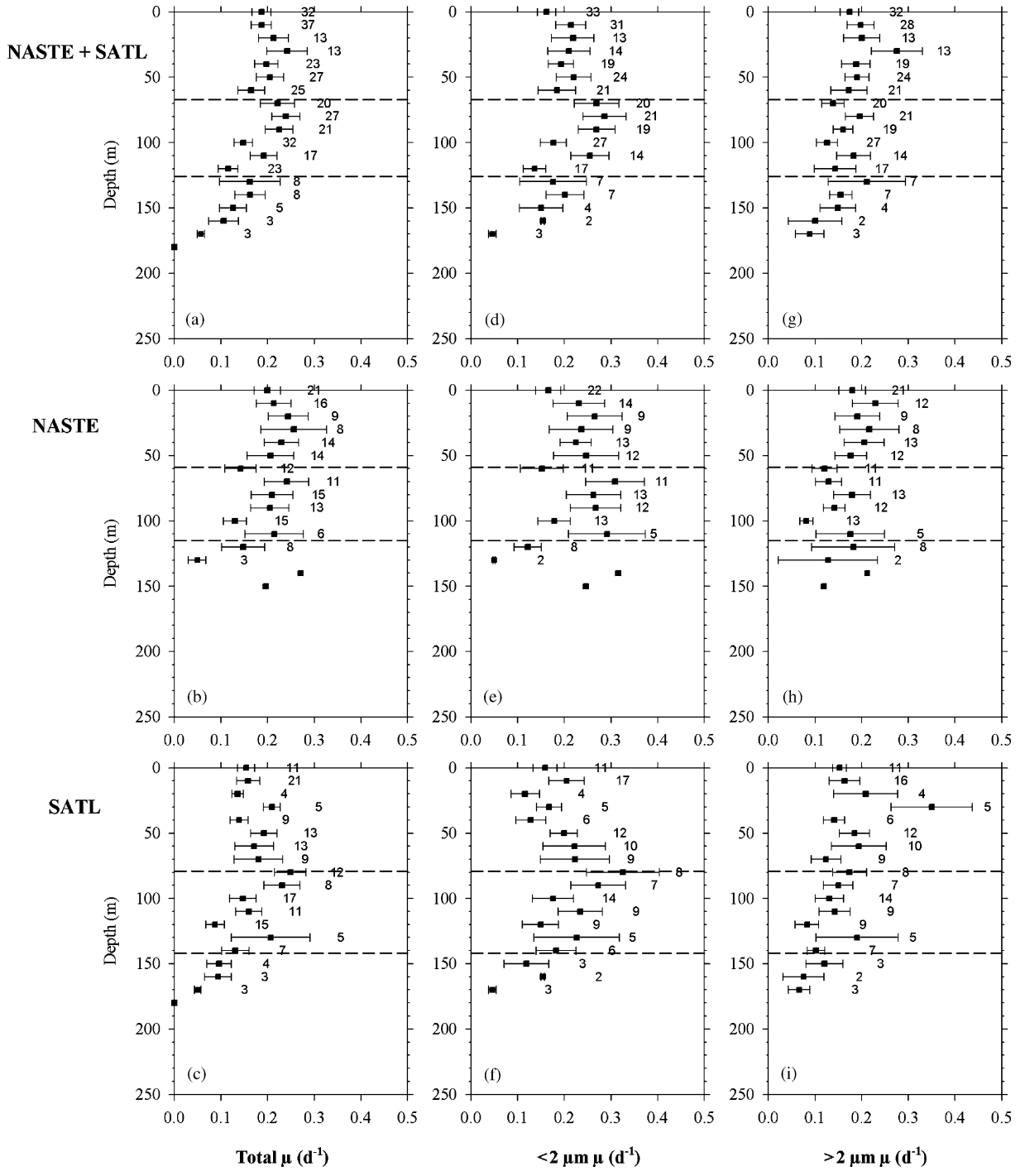

Fig. 5. Averaged vertical profiles of phytoplankton growth rates (μ, d^{-1}) for total phytoplankton (left panels), for the $<2\,\mu m$ phytoplankton size fraction (central panels) and for the $>2\,\mu m$ phytoplankton size fraction (right panels) at all sampling stations (a, d and g), at the stations located in the Northern gyre (b, e and h) and at the stations located in the Southern gyre (c, f and i). Horizontal bars represent the standard error (s.e.). Numbers indicate the number of values making up each average. No number (or error bar) indicates only a single value. Dashed lines represent the vertical limits of the DCML.

Table 4
Averaged integrated values ± standard error (s.e.) of selected variables in the upper mixed layer (ML) and in the DCM layer (DCML) for each size fraction in the NASTE and SATL regions

	Total fraction		<2 μm fraction		>2 μm fraction	
	Upper layer	DCM layer	Upper layer	DCM layer	Upper layer	DCM layer
NASTE						
Chl-*a* ($mg\,m^{-2}$)	4.6±0.3	12.2±0.8	2.9±0.2	9.0±0.6	1.6±0.1	2.9±0.2
	28±1%	**72±9%**	**26±1%**	**74±1%**	**36±2%**	**64±2%**
Est Phyto-C ($mg\,m^{-2}$)	472±29	395±25	226±15	206±14	302±23	217±15
	54±1 %	**46±1%**	**52±1%**	**48±1%**	**57±1%**	**43±1%**
Primary production ($mg\,m^{-2}\,d^{-1}$)	88±12	72±9	41±6	50±6	54±7	27±4
	54±2%	**46±2%**	**44±3%**	**56±3%**	**65±2%**	**35±2%**
SATL						
Chl-a ($mg\,m^{-2}$)	8.3±0.5	15.8±0.8	5.9±0.3	11.9±0.6	2.0±0.14	2.6±0.2
	35±2%	**65±2%**	**34±2%**	**66±2%**	**6±3 %**	**54±3%**
Est Phyto-C ($mg\,m^{-2}$)	854±49	514±25	452±25	279±14	372±23	194±16
	62±2%	**38±2%**	**61±2%**	**39±2%**	**65±2%**	**35±2%**
Primary production ($mg\,m^{-2}\,d^{-1}$)	115±11	83±10	64±7	53±7	56±6	29±4
	59±3%	**41±3 %**	**55±3%**	**45±3%**	**66±4%**	**34±4%**

Numbers in bold represent the averaged contribution (%) ± s.e. of each layer to the integrated value throughout the water column (ML + CML).

primary production, picoplankton growth rates were significantly higher in the DCML than in the ML (*t*-test, $p<0.001$).

3.4. Contribution of the DCM to the phytoplankton biomass and productivity of the Atlantic subtropical gyres

Phytoplankton carbon biomass and primary production were depth-integrated in the ML, in the DCML and throughout the water column (ML + DCML layer) to estimate the relative contribution of each layer to the total biomass and productivity of the subtropical gyres (Table 4). In the NASTE, the DCML accounted for the same fraction of the water column picoplankton biomass and primary production as the ML (*t*-test, $p>0.05$). For the large phytoplankton size fraction the DCML represented a significantly lower fraction of the water column primary production (35±2%; *t*-test, $p<0.001$) and biomass (43±1%; *t*-test, $p<0.001$). In the SATL, the ML layer showed significantly higher contributions to water column phytoplankton biomass and primary production than the DCML (~60%; *t*-test, $p<0.001$ for biomass and $p<0.05$ for primary production). The exception, in this region, was the small phytoplankton size fraction, where no significant differences were found between the contribution of the DCML and the ML to primary production (*t*-test, $p>0.05$).

4. Discussion

4.1. Vertical distribution of phytoplankton size fractions

The importance of small phytoplankton cells in the oligotrophic regions of the ocean is well established in terms of Chl-*a* concentrations, cell abundances and primary production rates (e.g., Zubkov et al., 1998; Marañón et al., 2001). However, the vertical pattern of the relative contribution of picoplankton to total phytoplankton biomass remains unclear. In the tropical Atlantic, Herbland et al. (1985) found that the contribution of the small (<1 μm) phytoplankton to total Chl-*a* was maximum (~70%) in the nitrate-depleted upper mixed layer (NO_3^- <0.1 μM), decreased to 50% at the nitracline depth and was always <50% in the nutrient-replete, light-limited bottom layer. The same vertical distribution of Chl-*a* <1 μm was observed in the equatorial Pacific by LeBouteiller et al. (1992), who identified <1 μm phytoplankton size with photosynthetic prokaryotes and >1 μm with eukaryotic microalgae, but they did not measure the abundances of these groups. Although small cells absorb light more efficiently in low-irradiance environments, as at the bottom of the euphotic layer in the tropical oceans, it seems that the influence of irradiance on phytoplankton vertical distribution in the tropical

oceans is less important than the effect of nutrient availability. These results suggest that the vertical distribution of phytoplankton in these areas is controlled largely by nutrient availability, as small phytoplankton cells are more efficient in taking up nutrients at low nutrient levels. In contrast, our study shows that the contribution of picoplankton ($<2\,\mu m$) to total Chl-*a* in the subtropical gyres increased with depth. Similar findings have been reported by Lutz et al. (2003) in the North Atlantic and Taguchi et al. (1988) in the Caribbean Sea and in the subtropical western Atlantic. Our results also agree with those of Gin et al. (1999) in the Sargasso Sea, who found an increase in the relative contribution of picoplankton cells down to the DCM depth and a slight shift towards large phytoplankton sizes, based on the slope of size-abundance spectrum, below the DCM. These authors explained the dominance of small cells at the DCM in terms of the competitive advantages of small-sized cells in reduced irradiance conditions.

The apparent discrepancy in the vertical distribution pattern of phytoplankton size structure is likely to be related to the different phytoplankton size fractions considered in the studies. In their investigations, Herbland et al. (1985) and LeBouteiller et al. (1992) used 1 μm as the upper limit for the picoplankton size class. According to Campbell and Vaulot (1993), *Prochlorococcus* cells (0.5–0.7 μm) dominated the ML, and picoeukaryotes, which are larger than 1 μm and therefore not included in the Herbland et al. (1985) and LeBouteiller et al. (1992) studies, dominated below the DCM. In general, the vertical distribution of *Prochlorococcus* in the subtropical Atlantic is homogeneous in the ML and presents a maximum close to the DCM depth, where this taxonomic group dominates in terms of carbon biomass, Chl-*a* and cell abundance (e.g., Zubkov et al., 1998). The vertical distribution of picoeukaryotes also shows increasing abundances with depth, reaching maximum values at the DCM, where they account for an important fraction of phytoplankton biomass (Li, 1995; Partensky et al., 1996; Veldhuis and Kraay, 2004).

4.2. C to Chl-a ratios

Measurement of phytoplankton carbon biomass in natural populations is not straightforward. During this study we obtained Phyto C on only two cruises from flow cytometry and microscopical count and identification. However, Chl-*a* was obtained routinely on all cruises. So we decided to convert the easily measured Chl-*a* to carbon by means of appropriate C:Chl-*a* ratio as an alternative to the direct quantification of Phyto C. A wide range of C:Chl-*a* ratios, from ca. 20 to >400, has been reported in phytoplankton cultures growing at different rates under different nutrient availability, light, and temperature conditions (Laws and Bannister, 1980; Sakshaug et al., 1989; Geider, 1993). The different patterns followed by the vertical distributions of Phyto C and Chl-*a* observed in this study suggested the C:Chl-*a* ratio might vary with depth. So, we calculated the corresponding C:Chl-*a* ratios for each depth where both variables were concurrently measured. The averaged (±s.e.) C:Chl-*a* ratio was 103±7 (ranging from 56 to 200) in the ML and 24±4 (ranging from 11 to 54) in the DCML, when the data sets from both gyres were jointly considered. Our C:Chl-*a* estimates for the ML are slightly lower than those previously reported in the eastern subtropical North Atlantic (~160–250; Taylor et al., 1997; Veldhuis and Kraay, 2004; Behrenfeld et al., 2005). The C:Chl-*a* ratios estimated for the western subtropical North Atlantic by different authors were more variable, ranging from 40–160 in the ML to 15–65 in the DCML (Li et al., 1992; Goericke and Welschmeyer, 1998; Lefèvre et al., 2003). This wide range of values is probably related to the different methods used in these studies (Marañón, 2005) and to the larger seasonal variability characteristic of the upper water column in the western subtropical Atlantic (e.g., Longhurst, 1998). It is noteworthy that, despite the differences in magnitude, all the studies carried out in subtropical and tropical oceans show that C:Chl-*a* ratios are always 3–6 fold higher in surface waters than at the DCM (Malone et al., 1993; Campbell et al., 1994; Veldhuis and Kraay, 2004), which reflects the increasing chlorophyll content per cell as irradiance levels decrease, as has been reported for *Synechococcus* and *Prochlorococcus* (Olson et al., 1990; Campbell and Vaulot, 1993; Lutz et al., 2003).

In this study, we also observed differences in the C:Chl-*a* ratios as a function of phytoplankton size. We estimated higher ratios in the $>2\,\mu m$ than in the $<2\,\mu m$ size fraction (Table 3). These results, however, must be taken with caution, as phytoplankton C biomass was estimated by different methods for the two size fractions (see Section 2). Although the comparison of our results is difficult, mainly because of the size classes considered in our study and to the different methods used in the

literature to estimate phytoplankton biovolumes and carbon content, previous field and culture studies have also reported an increase in C:Chl-*a* ratio with phytoplankton size (Furuya, 1990; Finkel, 2001; Arin et al., 2002). This is expected on theoretical grounds, since pigment content is more closely related to cell surface area, whereas carbon content is more closely related to cell volume (Finkel, 2001). However, other studies show that the C:Chl-*a* ratio does not change with cell size (Blasco et al., 1982; Geider et al., 1986; Montagnes et al., 1994). Besides, we cannot rule out the possibility that the size dependence of the C:Chl-*a* ratio could be related to differences in taxonomic composition between small ($<2\,\mu m$) and large ($>2\,\mu m$) phytoplankton. Thus, prokaryote phytoplankton usually show higher C:Chl-*a* ratios than eukaryotes (Furuya, 1990; Odate et al., 1993; Geider, 1993), and also dinoflagellates have been reported to show higher ratios as compared to diatoms grown in cultures (Chan, 1980).

Nevertheless, it is necessary to note that our results could be biased by the use of constant C/cell conversion factors to estimate picoplankton carbon content from cell abundances (see Section 2). It is well known that, in the subtropical gyres, *Prochlorococcus*, *Synechococcus* and picoeukaryotic cell sizes (Li et al., 1992; Sieracki et al., 1995), and therefore the carbon content per cell, change with depth. In order to check the effect of the vertical variability of this factor on our results we applied different C/cell factors obtained from the literature to our picoplankton abundances. We estimated *Prochloroccus* and *Synechococcus* biomass by assuming the conversion factors reported by Sieracki et al. (1995) in the Sargasso Sea: 10 fg C/cell in the ML and 49 fg C/cell in the DCML for *Prochlorococcus* and 99 fg C/cell in the ML and 199 fg C/cell in the DCML for *Synechococcus*. For picoeukaryotes a constant factor 1500 fg C/cell (Zubkov et al., 1998) was used, despite the fact that this group shows a slight decrease of cell size with depth (Li et al., 1992; Xelu Morán, pers. commun.). With these factors we obtained lower C:Chl-*a* ratios for the small size fraction (39 in the ML and 25 in the DCML) and for the total size fraction (77 in the ML and 30 in the DCML) than those obtained assuming a constant factor with depth (see Table 3). However, the C:Chl-*a* ratios are still higher in the ML than in the DCML (*t*-test, $p<0.05$ for the small size fraction and $p<0.001$ for the total size fraction). Recently, Veldhuis and Kraay (2004) used a slightly higher conversion factor for *Prochlorococcus* (35 fg C/cell in the ML and 50 fg C/cell in the DCML). Using these factors for *Prochlorococcus* and maintaining *Synechococcus* and picoeukaryotes factors as above we calculated C:Chl-*a* ratios and phytoplankton growth rates similar to those reported in our study. In any case, C:Chl-*a* ratios for picoplankton are higher in the ML than in the DCML, suggesting that the increase in the C/cell ratio with depth is lower than that of the Chl-*a*/cell ratio.

4.3. DCML contribution to phytoplankton biomass and productivity

In this study, the DCML, defined as depths where Chl-*a* concentrations are 0.5 times higher than the value measured at the Chl-*a* maximum, accounted for 65–75% of the euphotic-depth-integrated Chl-*a* concentration in the subtropical gyres of the Atlantic Ocean. However, our results show that, as reported in previous studies, the DCML does not represent either a phytoplankton biomass or a primary production maximum (Table 4; Claustre and Marty, 1995; Goericke and Welschmeyer, 1998; Marañón et al., 2000). Using photosynthesis-irradiance (P-E) experiments, Lorenzo et al. (2004) found a DCML contribution to primary production ($54\pm17\%$, average $\pm$ s.d.) similar to that reported in our study (46 ± 2, average $\pm$ s.e.) although these authors defined the DCML as the layer that showed a steady increase–decrease in the Chl-*a* concentration above and below of the maximum Chl-*a* value of the water column.

It is necessary to note that, although during our study the DCML accounted for a similar or slightly lower amount of the water-column-integrated primary production than the ML (Table 4), the highest primary production rates were measured well above the DCM (Figs. 4a and b). These results suggest that the reduced light environment at the DCM depth may be partially compensated by an increase in the chlorophyll concentration, resulting in a contribution of the DCML to the water column integrated primary production similar to that of the ML. Therefore, it would be necessary to consider the Chl-*a* profile in primary productivity models.

4.4. Phytoplankton growth rates

There is a growing interest in the estimation of phytoplankton growth rates in the ocean as they

largely determine the degree of coupling between autotrophic and heterotrophic components of the planktonic community (Marañón et al., 2000) and therefore affect the carbon fluxes through the planktonic food web. Observed phytoplankton growth rates in the oligotrophic oceans are either close to their theoretical maximum values, i.e., 1.5–2 d^{-1} in the subtropical Pacific (Laws et al., 1984, 1987; Jones et al., 1996), or well below these values in the subtropical North Atlantic (Malone et al., 1993; Goericke and Welschmeyer, 1998; Marañón et al., 2000). Phytoplankton growth rates estimated in the upper layer of the subtropical Atlantic during our study (averaged value of 0.17 d^{-1}) were lower than those previously reported in the eastern subtropical North Atlantic (0.4–0.8 d^{-1}; Stelfox-Widdicombe et al., 2000; Quevedo and Anadón, 2001) and in the lower end of the range reported in the western subtropical Atlantic (0.1 −1.3 d^{-1}; Malone et al., 1993; Goericke and Welschmeyer, 1998; Lessard and Murrell, 1998).

The low phytoplankton growth rates presented here are a direct consequence of the primary production rates and phytoplankton biomass estimated in our study. Averaged euphotic-depth-integrated primary production rates measured in the NASTE and SATL (156 ± 16 and 205 ± 17 mg C m^{-2} d^{-1}, respectively) are lower than those reported in other oligotrophic areas such as the Bermuda Atlantic and Hawaii Ocean time-series (BATS and HOT, respectively, with an annual averaged rate ~500 mg C m^{-2} d^{-1}) and slightly lower than those estimated with the bio-optical model of Longhurst et al. (1995; 330 and 210 mg C m^{-2} d^{-1} in the NASTE and SATL, respectively). However, differences between these areas could be explained by taking into account their hydrographic characteristics. The HOT zone in the subtropical Pacific is a permanently stratified region with mixed layer depth nearly always $\ll$100 m, and therefore lower primary production rates than in the subtropical North Atlantic could be expected. However, other factors, such as the availability of dissolved inorganic phosphate, which is much lower in the subtropical North Atlantic than in the subtropical Pacific (Wu et al., 2000), could be influencing productivity differences between the two areas. The BATS station is located near the edge of the subtropical gyre and experiences deep mixing during winter months (100–400 m), leading to a modest spring bloom. Most of our data derive from AMT cruises carried out in May and October, and therefore, we could have missed high primary production events in late winter/early spring, which would be recorded in the BATS programme because of the monthly sampling. Nevertheless, averaged primary production rate from Bermuda time series in May and October from 1989 to 2001 (http://bats.bbsr.edu/) are still higher (472 ± 29 mg C m^{-2} d^{-1}, average ± se) than ours. Another important difference is the intense eddy activity in the BATS region (McGillicuddy et al., 1998), which has been suggested to represent an important nutrient input to the euphotic layer in the area in comparison to the eastern North Atlantic gyre, where we have never detected inorganic nutrients in surface waters.

It is necessary to take into account some processes that could be affecting our estimates of phytoplankton growth, such as losses of ^{14}C during primary production incubations due to the grazing, or the possible mixotrophic activity of the phytoplankton. Firstly, if during primary production experiments zooplankton respired or excreted a significant amount of the ^{14}C previously ingested as a consequence of their grazing activity, we would be underestimating primary production. Given that the small size of the incubation bottles used in our study (70 ml) exclude mesozooplankton, the effect of microzooplankton on primary production measurements could be estimated by using the model of Laws et al. (1984). Assuming that 70% of labelled carbon is respired or excreted by microzooplankton (Landry and Calbet, 2004), that grazing rate equals 99% of phytoplankton growth rate, and a phytoplankton growth rate close to the theoretical maximum of 2 d^{-1}, during a incubation of 6–7 h the model predict that microzooplankton activity would reduce by 17% the estimated ^{14}C particulate primary production. Therefore, if actual phytoplankton growth rates were that high, we would be underestimating primary production rates, because of the grazing activity, and consequently phytoplankton growth rates. However, these rates would still be lower than 0.25 d^{-1}. Secondly, as our growth estimates are based only on photosynthesis they may underestimate real growth rates if the use of organic substances by phytoplankton is widespread and significant. Recent studies show that *Prochlorococcus* spp. are able to use organic nitrogen compounds in the oligotrophic open ocean (Zubkov et al., 2003). These authors estimated that amino-acid uptake represents 10% of the nitrogen requirements of *Prochloroccocus* in oligotrophic areas

assuming that *Prochlorococcus* accounts for 50% of the total primary production and 30% of the leucine-derived bacterioplankton production, and a C:N ratio of 6.6 for this group. Taking into account these values the amino-acid uptake of *Prochloroccocus* in their study represents 5% of total primary production. These estimates suggest that the use of amino acids is small in comparison with the use of inorganic carbon. Mixotrophy is also common among flagellates. During our study, we have included unidentified flagellate biomass of unclear trophic status into the Phyto C. We checked the effect of considering different contributions of autotrophs to total unidentified flagellates on C:Chl-*a* ratios. We found that it suffices that autotrophs represent $\geqslant 30\%$ of the unidentified flagellates in the ML (or 15% in the DCML) for the resulting C:Chl-*a* ratios to be higher in large than in small phytoplankton. Besides, a smaller contribution of autotrophs would imply total C:Chl-*a* ratios lower than those typically reported in the literature (for example, a contribution $<30\%$ would result in C:Chl-*a* ratios of 76 ± 4 in the ML and 20 ± 3 in the DCML).

Slow phytoplankton growth rates in the subtropical Atlantic have been explained in terms of the observed assimilation numbers and C:Chl-*a* ratios in a review by Marañón (2005). He estimated the maximum potential growth rate as $\mu_{max} = D \times P^{B}_{max}/C : \text{Chl-}a$ where P^{B}_{max} is the light-saturated, chlorophyll normalised photosynthesis rate, obtained in short (2 h) incubations (therefore minimising effects of ^{14}C respiration and bottle confinement) during the central hours of the day (when P^{B}_{max} is close to its maximum) and D is the duration of the photoperiod to convert hourly into daily rates. According to this equation, and given C:Chl-*a* from the literature, the P^{B}_{max} necessary to support phytoplankton growth rates of $1\,d^{-1}$ would be well above those reported in the subtropical Atlantic. The low phytoplankton growth rates measured in our study, together with the low heterotrophic bacteria growth rates reported for the upper waters of the subtropical Atlantic gyres (e.g. $0.12\,d^{-1}$; Zubkov et al., 2000), suggest the existence of a microbial community that turns over very slowly.

Small phytoplankton presented higher (*t*-test, $p<0.001$) growth rates in the DCML ($0.25\pm0.02\,d^{-1}$) than in the ML ($0.18\pm0.01\,d^{-1}$), while the contrary (*t*-test, $p<0.05$) occurred in the larger size fraction ($0.16\pm0.01\,d^{-1}$ at ML vs. $0.13\pm0.01\,d^{-1}$ at the DCML). Our results suggested that picoplankton might outcompete large cells in high-nutrient, low-light environment of the DCML. Although to our knowledge there are no studies reporting in-situ phytoplankton growth rates for different size classes, we can compare our picoplankton growth rates with those of *Prochlorococcus*, as this species is the main component of picoplankton in our study area. Our estimates agree with those of Goericke and Welschmeyer (1998) in the upper layer of Sargasso Sea; they measured *Prochlorococcus* growth rates of $0.2–0.3\,d^{-1}$ using the ^{14}C labelling of divinyl Chl-*a*. However, *Prochlorococcus* growth rates above the maximum values measured in cultures (from 0.5 to $0.6\,d^{-1}$; Partensky et al., 1999) were estimated in the subtropical Pacific ($0.2–0.6\,d^{-1}$) and in the Arabian Sea (up to $1\,d^{-1}$) by cell cycle analysis (Liu et al., 1997; Liu et al., 1998).

5. Conclusions

We have characterized the vertical variability of phytoplankton biomass, size structure, production and growth in the Atlantic subtropical gyres. In answer to the questions posed in the Introduction, we concluded that: (1) picophytoplankton contribution to total Chl-*a* and primary production increased with depth to the DCM; (2) the deep chlorophyll maximum does not represent a phytoplankton-biomass or primary-productivity maximum but contributes a substantial fraction of the vertically integrated algal standing stocks and C-fixation rates; and (3) phytoplankton grew at the same slow rate in the DCML as in the ML.

Acknowledgments

Thanks are given to Derek Harbour for providing data on phytoplankton abundance and biomass. Comments by Alex Poulton and three anonymous reviewers improved an early version of the manuscript. We are indebted to the Captain and crew of the research vessels, as well as to all colleagues on board during the 10 cruises. This study was supported by the UK Natural Environment Research Council through the Atlantic Meridional Transect programme (NER/O/S/2001/00680), the EU Contract CANIGO (MAS3CT960060), and a grant from the Spanish Ministry of Science and Technology (McyT) (CIRCANA, MAR99-1072-01). V.P. was supported by a postgraduate

fellowship from the MCyT. This is AMT contribution 109.

References

Arin, L., Morán, X.A.G., Estrada, M., 2002. Phytoplankton size distribution and growth rates in the Alboran Sea (SW Mediterranean): short term variability related to mesoscale hydrodynamics. Journal of Plankton Research 24 (10), 1019–1033.

Barlow, R.G., Aiken, J., Holligan, P.M., Cummings, D.G., Maritorena, S., Hooker, S., 2002. Phytoplankton pigment and absorption characteristics along meridional transects in the Atlantic Ocean. Deep-Sea Research I 49 (4), 637–660.

Behrenfeld, M.J., Boss, E., Siegel, D.A., Shea, D.M., 2005. Carbon-based ocean productivity and phytoplankton physiology from space. Global Biogeochemical Cycles 19.

Blasco, D., Packard, T.T., Garfield, P.C., 1982. Size dependence of growth rate, respiratory electron transport system activity, and chemical composition in marine diatoms in the laboratory. Journal of Phycology 18 (1), 58–63.

Campbell, L., Nolla, H.A., Vaulot, D., 1994. The importance of *Prochlorococcus* to community structure in the central North Pacific Ocean. Limnology and Oceanography 39 (4), 954–961.

Campbell, L., Vaulot, D., 1993. Photosynthetic picoplankton community structure in the subtropical North Pacific Ocean near Hawaii (Station ALOHA). Deep-Sea Research I 40 (10), 2043–2060.

Chan, A.T., 1980. Comparative physiological study of marine diatoms and dinoflagellates in relation to irradiance and cell size. II. Relationship between photosynthesis, growth, and carbon/chlorophyll *a* ratio. Journal of Phycology 16 (3), 428–432.

Claustre, H., Marty, J.C., 1995. Specific phytoplankton biomasses and their relation to primary production in the tropical North Atlantic. Deep-Sea Research I 42 (8), 1475–1493.

Cullen, J.J., 1982. The deep chlorophyll maximum: comparing vertical profiles of chlorophyll *a*. Canadian Journal of Fisheries and Aquatic Sciences 39 (5), 791–803.

Finkel, Z.V., 2001. Light absorption and size scaling of light-limited metabolism in marine diatoms. Limnology and Oceanography 46 (1), 86–94.

Furuya, K., 1990. Subsurface chlorophyll maximum in the tropical and subtropical western Pacific Ocean: vertical profiles of phytoplankton biomass and its relationship with chlorophyll *a* and particulate organic carbon. Marine Biology 107 (3), 529–539.

Geider, R.J., 1993. Quantitative phytoplankton physiology: implications for primary production and phytoplankton growth. ICES Marine Science Symposium 197, 52–62.

Geider, R.J., Platt, T., Raven, J.A., 1986. Size dependence of growth and photosynthesis in diatoms: a synthesis. Marine Ecology Progress Series 30 (1), 93–104.

Gieskes, W.W., Kraay, G.W., 1986. Floristic and physiological differences between the shallow and the deep nanophytoplankton community in the euphotic zone of the open tropical Atlantic revealed by HPLC analysis of pigments. Marine Biology 91 (4), 567–576.

Gin, K.Y.H., Chisholm, S.W., Olson, R.J., 1999. Seasonal and depth variation in microbial size spectra at the Bermuda Atlantic time series station. Deep-Sea Research I 46 (7), 1221–1245.

Goericke, R., Welschmeyer, N.A., 1998. Response of Sargasso Sea phytoplankton biomass, growth rates and primary production to seasonally varying physical forcing. Journal of Plankton Research 20 (12), 2223–2249.

Gould, R.W., 1987. The deep chlorophyll maximum in the world ocean: a review. The Biologist 66 (1–4), 4–13.

Herbland, A., LeBouteiller, A., Raimbault, P., 1985. Size structure of phytoplankton biomass in the equatorial Atlantic Ocean. Deep-Sea Research A 32 (7), 819–836.

Herbland, A., Voituriez, B., 1979. Hydrological structure-analysis for estimating the primary production in the tropical Atlantic Ocean. Journal of Marine Research 37 (1), 87–101.

Holligan, P.M., Harris, R.P., Newell, R.C., Harbour, D.S., Linley, E.A.S., Lucas, M.I., Tranter, P.R.G., Weekley, C.M., 1984. Vertical distribution and partitioning of organic carbon in mixed, frontal and stratified waters of the English Channel. Marine Ecology Progress Series 14 (2–3), 111–127.

Holm-Hansen, O., Lorenzen, C., Holmes, R., Strickland, J., 1965. Fluorometric determination of chlorophyll. Journal de Conseil International Pour l'Exploration de la Mer 30 (1), 3–15.

Jones, D.R., Karl, D.M., Laws, E.A., 1996. Growth rates and production of heterotrophic bacteria and phytoplankton in the North Pacific subtropical gyre. Deep-Sea Research I 43 (10), 1567–1580.

Landry, M.R., Calbet, A., 2004. Microzooplankton production in the oceans. ICES Journal of Marine Science 61, 501–507.

Laws, E.A., Bannister, T.T., 1980. Nutrient- and light-limited growth of *Thalassiosira fluviatilis* in continuous culture, with implications for phytoplankton growth in the ocean. Limnology and Oceanography 25 (3), 457–473.

Laws, E.A., DiTullio, G.R., Redalje, D.G., 1987. High phytoplankton growth and production rates in the North Pacific subtropical gyre. Limnology and Oceanography 32 (4), 905–918.

Laws, E.A., Redalje, D.G., Haas, L.W., Bienfang, P.K., Eppley, R.W., Harrison, W.G., Karl, D.M., Marra, J., 1984. High phytoplankton growth and production-rates in oligotrophic Hawaiian coastal waters. Limnology and Oceanography 29 (6), 1161–1169.

LeBouteiller, A., Blanchot, J., Rodier, M., 1992. Size distribution patterns of phytoplankton in the western Pacific: towards a generalization for the tropical open ocean. Deep-Sea Research A 39 (5A), 805–823.

Lefèvre, N., Taylor, A.H., Gilbert, F.J., Geider, R.G., 2003. Modeling carbon to nitrogen and carbon to chlorophyll a ratios in the ocean at low latitudes: evaluation of the role of physiological plasticity. Limnology and Oceanography 48 (5), 1796–1807.

Lessard, E.J., Murrell, M.C., 1998. Microzooplankton herbivory and phytoplankton growth in the northwestern Sargasso Sea. Aquatic Microbial Ecology 16 (2), 173–188.

Letelier, R.M., Dore, J.E., Winn, C.D., Karl, D.M., 1996. Seasonal and interannual variations in photosynthetic carbon assimilation at Station ALOHA. Deep-Sea Research II 43 (2–3), 467–490.

Li, W.K.W., 1995. Composition of ultraphytoplankton in the central North Atlantic. Marine Ecology Progress Series 122 (1–3), 1–8.

Li, W.K.W., Dickie, P.M., Irwin, B.D., Wood, A.M., 1992. Biomass of bacteria, cyanobacteria, prochlorophytes and photosynthetic eukaryotes in the Sargasso Sea. Deep-Sea Research A 39 (3–4A), 501–519.

Liu, H., Campbell, L., Landry, M.R., Nolla, H.A., Brown, S.L., Constantinou, J., 1998. Prochlorococcus and Synechococcus growth rates and contributions to production in the Arabian Sea during the 1995 Southwest and Northeast Monsoons. Deep-Sea Research II 45 (10–11), 2327–2352.

Liu, H., Nolla, H.A., Campbell, L., 1997. Prochlorococcus growth rate and contribution to primary production in the equatorial and subtropical North Pacific Ocean. Aquatic Microbial Ecology 12 (1), 39–47.

Longhurst, A., 1998. Ecological Geography of the Sea. Academic Press, New York.

Longhurst, A., Sathyendranath, S., Platt, T., Caverhill, C., 1995. An estimate of global primary production in the ocean from satellite radiometer data. Journal of Plankton Research 17, 1245–1271.

Lorenzo, L.M., Figueiras, F.G., Tilstone, G.H., Arbones, B., Mirón, I., 2004. Photosynthesis and light regime in the Azores Front region during summer: are light-saturated computations of primary production sufficient? Deep-Sea Research I 51 (9), 1229–1244.

Lutz, V.A., Sathyendranath, S., Head, E.J.H., Li, W.K.W., 2003. Variability in pigment composition and optical characteristics of phytoplankton in the Labrador Sea and the Central North Atlantic. Marine Ecology Progress Series 260, 1–18.

Malone, T.C., Pike, S.E., Conley, D.J., 1993. Transient variations in phytoplankton productivity at the JGOFS Bermuda time series station. Deep-Sea Research I 40 (5), 903–924.

Marañón, E., 2005. Phytoplankton growth rates in the Atlantic subtropical gyres. Limnology and Oceanography 50 (1), 299–310.

Marañón, E., Holligan, P.M., Barciela, R., González, N., Mouriño, B., Pazó, M.J., Varela, M., 2001. Patterns of phytoplankton size structure and productivity in contrasting open-ocean environments. Marine Ecology Progress Series 216, 43–56.

Marañón, E., Holligan, P.M., Varela, M., Mouriño, B., Bale, A.J., 2000. Basin-scale variability of phytoplankton biomass, production and growth in the Atlantic Ocean. Deep-Sea Research I 47 (5), 825–857.

Marra, J., Barber, R.T., 2004. Phytoplankton and heterotrophic respiration in the surface layer of the ocean. Geophysical Research Letters 31.

McGillicuddy, D.J., Robinson, A.R., Siegel, D.A., Jannasch, H.W., Johnson, R., Dickey, T.D., McNeil, J., Michaels, A.F., Knap, A.H., 1998. Influence of mesoescale eddies on new production in the Sargasso Sea. Nature 394, 263–266.

Montagnes, D.J.S., Berges, J.A., Harrison, P.J., Taylor, F.J.R., 1994. Estimating carbon, nitrogen, protein, and chlorophyll *a* from volume in marine phytoplankton. Limnology and Oceanography 39 (7), 1044–1060.

Morán, X.A.G., Fernández, E., Pérez, V., 2004. Size-fractionated primary production, bacterial production and net community production in subtropical and tropical domains of the oligotrophic NE Atlantic in autumn. Marine Ecology Progress Series 274, 17–29.

Odate, T., Yanada, M., Mizuta, H., Maita, Y., 1993. Phytoplankton carbon biomass estimated from the size-fractionated chlorophyll *a* concentration and cell density in the northern coastal waters from spring bloom to summer. Bulletin of Plankton Society of Japan 39 (2), 127–144.

Olson, R.J., Chisholm, S.W., Zettler, E.R., Altabet, M.A., Dusenberry, J.A., 1990. Spatial and temporal distributions of prochlorophyte picoplankton in the North Atlantic Ocean. Deep-Sea Research A 37 (6), 1033–1051.

Ondrusek, M.E., Bidigare, R.R., Sweet, S.T., Defreitas, D.A., Brooks, J.M., 1991. Distribution of phytoplankton pigments in the North Pacific Ocean in relation to physical and optical variability. Deep-Sea Research A 38 (2), 243–266.

Ondrusek, M.E., Bidigare, R.R., Waters, K., Karl, D.M., 2001. A predictive model for estimating rates of primary production in the subtropical North Pacific Ocean. Deep-Sea Research II 48 (8–9), 1837–1863.

Partensky, F., Blanchot, J., Lantoine, F., Neveux, J., Marie, D., 1996. Vertical structure of picophytoplankton at different trophic sites of the tropical northeastern Atlantic Ocean. Deep-Sea Research I 43 (8), 1191–1213.

Partensky, F., Hess, W.R., Vaulot, D., 1999. *Prochlorococcus*, a marine photosynthetic prokaryote of global significance. Microbiology and Molecular Biology Reviews 63 (1), 106–127.

Quevedo, M., Anadón, R., 2001. Protist control of phytoplankton growth in the subtropical north-east Atlantic. Marine Ecology Progress Series 221, 29–38.

Sakshaug, E., Andresen, K., Kiefer, D.A., 1989. A steady state description of growth and light absorption in the marine planktonic diatom *Skeletonema costatum*. Limnology and Oceanography 34 (1), 198–205.

Sathyendranath, S., Longhurst, A., Caverhill, C.M., Platt, T., 1995. Regionally and seasonally differentiated primary production in the North Atlantic. Deep-Sea Research I 42 (10), 1773–1802.

Sieracki, M.E., Haugen, E.M., Cucci, T.L., 1995. Overestimation of heterotrophic bacteria in the Sargasso Sea: direct evidence by flow and imaging cytometry. Deep-Sea Research I 42 (8), 1399–1409.

Stelfox-Widdicombe, C.E., Edwards, E.S., Burkill, P.H., Sleigh, M.A., 2000. Microzooplankton grazing activity in the temperate and sub-tropical NE Atlantic: summer 1996. Marine Ecology Progress Series 208, 1–12.

Taguchi, S., DiTullio, G.R., Laws, E.A., 1988. Physiological characteristics and production of mixed layer and chlorophyll maximum phytoplankton populations in the Caribbean Sea and western Atlantic Ocean. Deep-Sea Research A 35 (8), 1363–1377.

Taylor, A.H., Geider, R.J., Gilbert, F.J.H., 1997. Seasonal and latitudinal dependencies of phytoplankton carbon-to-chlorophyll *a* ratios: results of a modelling study. Marine Ecology Progress Series 152 (1–3), 51–66.

Teira, E., Mouriño, B., Marañón, E., Pérez, V., Pazó, M.J., Serret, P., de Armas, D., Escánez, J., Woodward, E.M.S., Fernández, E., 2005. Variability of chlorophyll and primary production in the Eastern North Atlantic Subtropical Gyre: potential factors affecting phytoplankton activity. Deep-Sea Research I 52, 569–588.

Tréguer, P., LeCorre, P., 1975. Manuel d'analyse des sels nutritifs dans l'eau de mer (Utilisation de l'Autoanalyzer II Technicon (R)), 2ème Ed. Laboratoire d'Oceanologie Chimique, Universitè de Bretagne Occidentale, Brest.

Veldhuis, M.J.W., Kraay, G.W., 2004. Phytoplankton in the subtropical Atlantic Ocean: towards a better assessment of

biomass and composition. Deep-Sea Research I 51 (4), 507–530.

Venrick, E.L., 1999. Phytoplankton species structure in the central North Pacific, 1973–1996: variability and persistence. Journal of Plankton Research 21 (6), 1029–1042.

Welschmeyer, N.A., 1994. Fluorometric analysis of chlorophyll *a* in the presence of chlorophyll *b* and pheopigments. Limnology and Oceanography 39 (8), 1985–1992.

Woodward, E.M.S., 1994. Nutrient Analysis Techniques. Plymouth Marine Laboratory.

Wu, J.F., Sunda, W., Boyle, E.A., Karl, D.M., 2000. Phosphate depletion in the western North Atlantic Ocean. Science 289, 759–762.

Zubkov, M.V., Sleigh, M.A., Burkill, P.H., Leakey, R.J.G., 2000. Picoplankton community structure on the Atlantic Meridional Transect: a comparison between seasons. Progress in Oceanography 45 (3–4), 369–386.

Zubkov, M.V., Sleigh, M.A., Tarran, G.A., Burkill, P.H., Leakey, R.J.G., 1998. Picoplanktonic community structure on an Atlantic transect from 50°N to 50°S. Deep-Sea Research I 45 (8), 1339–1355.

Zubkov, M.V., Fuchs, B.M., Tarran, G.A., Burkill, P.H., Amann, R., 2003. High rate of uptake of organic nitrogen compounds by *Prochlorococcus* cyanobacteria as a key to their dominance in oligotrophic oceanic waters. Applied and Environmental Microbiology 69 (2), 1299–1304.